Ion Adsorption and Ion Exchange in Ultrathin Films of Fatty Acids

Dong June Ahn and Elias I. Franses
School of Chemical Engineering, Purdue University, West Lafayette, IN 47907

Ion exchange equilibria of ultrathin Langmuir and Langmuir-Blodgett films of stearic and arachidic acids in contact with aqueous electrolyte solutions were studied experimentally and theoretically. A model considering electrochemical and thermodynamic aspects of the adsorption of protons, calcium, and cadmium ions from solution to the film has been developed. Key parameters are the binding constants (K's) of ions and the mixing characteristics (or Flory-Huggins interaction parameters χ's) of ions in the two-dimensional film lattice plane. The ternary system can be described by the parameter values determined with binary proton-calcium ion, proton-cadmium ion, and calcium-cadmium ion systems: $K_{Ca}=2.9\times10^2$, $K_{Cd}=8.6\times10^3$, $K_H=3.6\times10^6$, $\chi_{H-Ca}=-0.76$, $\chi_{H-Cd}=0.13$, and $\chi_{Ca-Cd}=1.0$. Competitive ion adsorption was measured by FTIR ATR spectroscopy of either collapsed or ordered LB films. Data for the proton-calcium-cadmium ion system agreed well with the model predictions. The results show possible future applications of such thin films as ion sensors or ion exchange materials.

Introduction

Ultrathin films of organic materials have received much attention in several science and engineering fields (Swalen et al., 1987; Stroeve and Franses, 1987; Roberts, 1990; Ulman, 1991). During the last decade, many attempts have been made to develop engineering applications using thin films. Promising application areas are:

- Nonlinear optical and light-harvesting polymer systems (Swalen, 1986; Williams, 1988; Fox et al., 1993) utilizing oriented chromophores inducing directional electron transfer, for conversion of light energy into information and chemical energy

- Corrosion-barriers, passivating films, or membranes for separation or selective permeation of gas and liquid substances (Kuan et al., 1988; Bruinsma et al., 1992), since transport properties of such films are controlled by their thickness and micro (or nano) structure

- Sensors for detecting chemical and biological substances (Wohltjen et al., 1985; Moriizumi, 1988; Hua et al., 1990), since they use unique interactions of film materials with foreign species

- Molecularly engineered mono or multilayers for altering solid surfaces and controlling surface or interparticle forces (Whitesides and Laibinis, 1990; Chapman, 1993).

In this study, we report some interesting properties of thin films which may lead to ion exchange materials or better understanding of ion exchangers, with precise control of surface charge density.

When insoluble (Langmuir) monolayers of fatty or alkanoic acids are spread at the air/water interface, they interact strongly with bivalent or multivalent metal ions. Previous studies for binary ionic systems related certain ion adsorption characteristics only to the binding (or adsorption) constants of the ions. Yamauchi et al. (1968) and Petrov et al. (1982) used chemical equilibrium reaction models with the assumption that the Langmuir monolayer is neutral in charge. By contrast, McLaughlin et al. (1981), Löche et al. (1985), Pezron et al. (1990), and Bloch and Yun (1990) indicated that the Langmuir monolayer is electrically charged due to partial dissociation of the polar groups of the monolayer. They developed several electrochemical models that use a Langmuir isotherm for adsorption in the Stern layer and consider the electrical diffuse layer. Their models could account for ion binding of certain ions but not others. Experimental evidence amply indicated a need for improving the models (Deamer et al., 1967; Petrov et al., 1982; Kobayashi et al., 1988). Recently, it was found by Ahn and Franses (1991) that binary ion adsorption onto

the Langmuir monolayer is affected not only by the binding constant at the surface, which can quite differ from that in the bulk, but also by the mixing behavior of ions in the two-dimensional ionic layer binding to the monolayer. This mixing of ions was modeled well by a lattice model using Flory-Huggins binary interaction parameters.

In this article, we report new data on binary and ternary systems and develop a multicomponent model. The best-quality Langmuir-Blodgett (LB) films of salts of fatty acids are produced with bivalent ions such as calcium and cadmium. As our model ion exchange system, we have chosen an aqueous solution containing these ions and protons interacting with a Langmuir monolayer, in which the surface site density can be controlled precisely. The Langmuir monolayers were transferred from the air/water interface to ATR (attenuated total reflection) plates, dried, and subsequently analyzed by FTIR (Fourier Transform Infrared) ATR spectroscopy. Accordingly, the model was modified to account for minor composition changes upon the film transfer. Model calculations for this ternary ionic system were made with parameters determined from the binary ionic systems and compared with IR data.

Materials and Experimental Methods

Stearic acid (>99 wt. % pure, C_{18}), arachidic acid ($>99\%$, C_{20}), $CaCl_2 \cdot 2H_2O$ ($>99\%$), $Ca(OH)_2$ ($>98\%$), and $CdCl_2$ ($>99.999\%$), purchased from Fluka, Baker, and Aldrich companies, were used without further purification. Distilled water was purified by a Millipore-Q water system. The final deionized water had an initial resistivity of 18 M$\Omega \cdot$cm.

Fatty acid monolayers were spread from hexane solution (1 mg/mL) on the surface of the aqueous subsolution, either in a Joyce-Loebl IV trough or a KSV minitrough located in a clean room. The subsolutions were not buffered. Deionized water had a pH of 5.5 ± 0.2 after overnight exposure to ambient air. Initially, subsolutions contained 5×10^{-4} M $CaCl_2$ (pH = 5.5) or 10^{-4} M $Ca(OH)_2$ (pH = 10 ± 0.4). $CdCl_2$ up to 4×10^{-3} M was dissolved into these solutions. About 30 min was allowed for each solution to equilibrate, before other steps were followed.

ATR plates were used for sampling Langmuir monolayers. The Ge ATR plates were cleaned from organic impurities by immersing successively (under sonication at 58°C) in solutions of ethanol, trichloroethylene, ethanol, deionized water, ethanol, trichloroethylene, ethanol, and deionized water for 5 to 10 min per solution. The plates were finally rinsed with bulk deionized water at room temperature and dried by an Ar gas stream.

Langmuir monolayers were sampled at 22°C by vertical LB deposition on Ge ATR plates, at a dipping speed of 10 mm/ min and at surface pressures of 10 and 25 mN/m. Transfer ratios were close to unity. In another deposition method, monolayers were compressed beyond the collapse point (surface pressure higher than 45 mN/m) and then deposited by manually lifting the Ge ATR plate several times through the film to produce randomly oriented films. Pure fatty acid LB monomolecular films on pure water were deposited on hydrophilic or hydrophobic Si ATR plates, the surfaces of which were treated (Ahn and Franses, 1992a).

The IR spectra were collected at 24°C with a Nicolet 800 FTIR spectrophotometer equipped with an MCT (mercury cad-
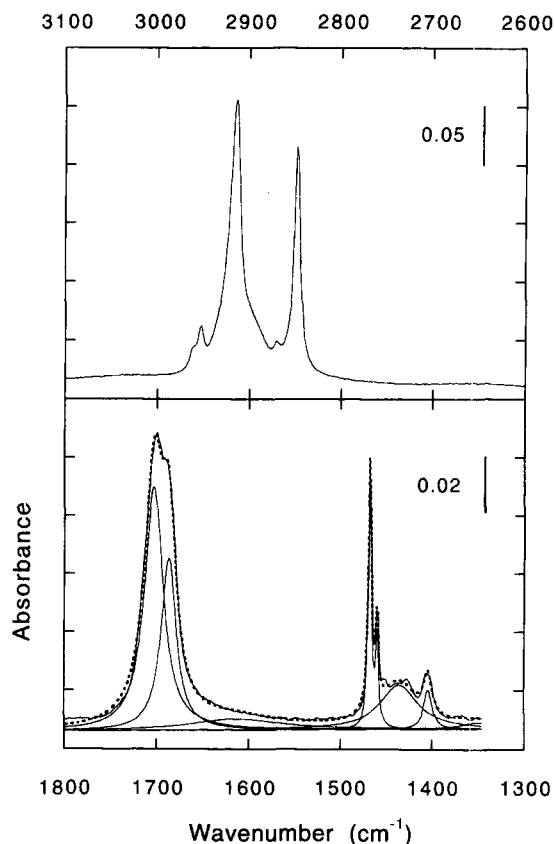

Figure 1. FTIR spectrum for stearic acid collapsed film.

Films were deposited on a Ge ATR plate from the aqueous subsolution of pH = 2.5: top, hydrocarbon stretch region; bottom, polar group stretch and hydrocarbon scissoring region. Region of the 1,800–1,350 cm^{-1} was fitted with fundamental peaks shown; the broken line is the sum of the fitted spectrum.

mium telluride) detector. The nominal spectral resolution was 2 cm^{-1}; 512 scans were taken for each sample. The films on Ge ATR plates were placed in the IR chamber for about 30 min for drying before the spectroscopic measurements were made. Nonpolarized FTIR spectra were usually obtained, unless indicated otherwise.

FTIR Spectroscopy for Analysis of Film Composition

FTIR spectra for stearic acid, calcium stearate, and cadmium stearate are shown in Figures 1, 2 and 3, respectively. For these films to be randomly oriented so that intensity depends only on density, not on orientation, they were prepared by depositing collapsed Langmuir monolayers, as detailed previously. The assignments of the hydrocarbon (CH) stretching region (3,100–2,700 cm^{-1}) have been given (Ahn and Franses, 1992a; Marshbanks et al., 1993). Absorbances in this region were used to determine relative film density. The band assignments in the 1,800–1,350 cm^{-1} region, which includes the polar groups C = O and COO$^-$, are given in Table 1. The spectra were fitted with a least-square method with fundamental peaks consisting of seven singlets and two doublets. The fundamental peaks were assumed to have Lorentzian lineshapes, which best characterize vibrational spectra, as opposed to Gaussian lineshapes. The fits satisfied the 95% confidence level and were visually good.
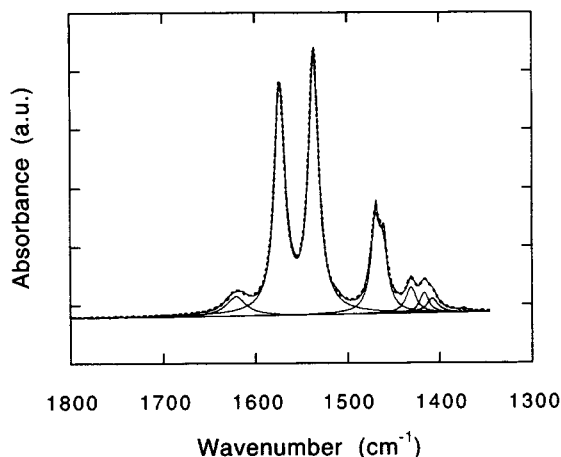
Figure 2. FTIR spectrum for calcium stearate collapsed film.

Subsolution had pH = 10 and $C_{Ca} = 10^{-4}$ M. The hydrocarbon stretch region is similar to that in Figure 1.

Table 1. Principal IR Bands in 1,800–1,350 cm⁻¹ Region*

Band	Peak Position	Fundamental Peak Used for Fitting
ν C=O	1,703 and 1,687**	Two singlets
H₂O	1,630–1,620	Singlet
ν^a COO-Ca	1,573 and 1,536	Doublet
ν^a COO-Cd	1,541	Singlet
δ CH₂	1,468 and 1,459	Doublet
ν^s COO, δ C$_\alpha$H₂	1,440–1,380†	Three singlets

* ν = stretching; ν^a = asymmetric stretching; ν^s = symmetric stretching, δ = scissoring. C$_\alpha$ indicates the carbon atom adjacent to carbonyl or carboxylic groups (Rabolt et al., 1983).

** Split is possibly due to Fermi resonance (Vogel et al., 1979) or due to the presence of two molecular conformations (Jain et al., 1989). Two singlets were used in spectral analyses.

† Combined bands were fitted with three singlets.

For the acid, the C = O stretching band can be resolved into two peaks at 1,703 and 1,687 cm⁻¹, the split possibly being due to a Fermi resonance (Vogel et al., 1979). The calcium salt shows a unique doublet at 1,573 and 1,536 cm⁻¹, which is assigned to the asymmetric stretching band of the COO⁻ group (Kimura et al., 1986). There is a corresponding symmetric stretching doublet in the region of 1,430–1,410 cm⁻¹. The intensity ratio of the 1,573 cm⁻¹ peak to the 1,536 cm⁻¹ peak is 0.9. The splits of the two bands are due to the presence of hydration water, the overtone band of which is located at 1,620 cm⁻¹. The COO⁻ asymmetric stretching band of the cadmium salt, which is not hydrated, is a singlet at 1,541 cm⁻¹. Hence, even though FTIR cannot be used for detecting calcium or cadmium ions directly, it can help one distinguish easily calcium stearate salt from cadmium stearate salt. The small peaks in the 1,440–1,380 cm⁻¹ region (see Table 1) are the combination of the symmetric carboxylate stretching band and the α-methylene scissoring band (Rabolt et al., 1983), and are
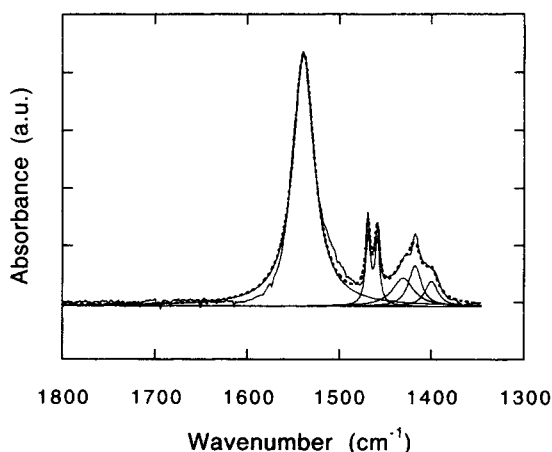
less important for the analysis. Three singlets used to fit these small peaks had little effect on the resulting compositions. Figure 4 shows a typical spectrum of a mixed film of calcium and cadmium stearate salts. The spectrum was fitted with the assumption that the calcium carboxylate asymmetric stretching doublet maintains the intensity ratio of the two peaks at 0.9, as found for the pure calcium salt case. The peak positions of the calcium and cadmium carboxylate bands were found to be the same in the mixture as in the pure salts. The carboxylate peaks apparently reflect only short-range chemical and electrical interactions of bound calcium and cadmium with carboxylate groups and are not likely to be affected by interactions with the neighboring molecules polar groups. In summary, the relative intensities of the acid, the calcium salt and the cadmium salt can be precisely determined (to within about 2%).

For the compositions to be determined from the relative polar group intensities, they need first to be properly normalized by the CH stretching intensities (which measure molecular density):

$$\alpha_i \equiv \frac{A_i}{A_{CH}} \quad (1)$$

Figure 3. FTIR spectrum for cadmium stearate collapsed film.

pH = 10 and $C_{Cd} = 10^{-4}$ M. The hydrocarbon stretch region is similar to that in Figure 1.
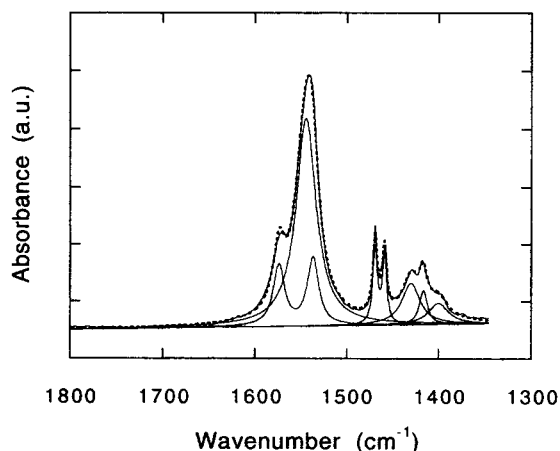

Figure 4. FTIR spectrum for mixed calcium and cadmium stearate collapsed film.

pH = 10, $C_{Ca} = 10^{-4}$ M, and $C_{Cd} = 3 \times 10^{-4}$ M.

Table 2. Comparison of Orientation and Composition in Collapsed and LB Films on Ge ATR Plates

Film Type*	pH	C_{Ca} (M)	C_{Cd} (M)	Π (mN/m)	Dichroic Ratio (2,849 cm^{-1})**	Chain Axis Orientation[†]	Composition		
							Φ_H	Φ_{Ca}	Φ_{Cd}
Cast	—	—	—	—	0.87	Random	1.00	0.00	0.00
Collapsed	2.5	0	0	—	0.88	Random	1.00	0.00	0.00
Collapsed	10	10^{-4}	0	—	0.89	Random	0.01	0.99	0.00
Collapsed	10	10^{-4}	10^{-6}	—	0.87	Random	0.00	0.84	0.16
Collapsed	10	10^{-4}	10^{-4}	—	0.88	Random	0.00	0.00	1.00
9-Layer LB (Y-Type)	10	10^{-4}	10^{-4}	10	0.93	$45 \pm 4°$	0.00	0.01	0.99
9-Layer LB (Y-Type)	10	10^{-4}	10^{-4}	25	0.95	$40 \pm 4°$	0.00	0.01	0.99

*Estimated thickness of cast film was about 0.2 μm. Absorbance intensities of collapsed films corresponded to those of 4 to 6 LB layers deposited on both sides of ATR plates, throughout the experiments in the present study.

**Dichroic ratio (± 0.01) is defined as the ratio of the absorbance intensity of TE wave (s-polarization) to that of TM wave (p-polarization), in the polarized FTIR ATR spectroscopy. Here, the symmetric methylene stretching band was used to calculate the dichroic ratios.

[†] As determined by Ahn and Franses (1992a); angle is average angle between chain axis and surface normal.

where A_i is the integrated absorbance of the band i, and i = H (acid), Ca (calcium salt), or Cd (cadmium salt). A_{CH} is the integrated CH stretching absorbance in the 3,050–2,750 cm^{-1}. Then, the composition Φ_i of the component i is related to the A_i value of each peak component:

$$\Phi_i = \frac{\alpha_i^{-1} A_i}{\sum_i \alpha_i^{-1} A_i} \qquad (2)$$

α_i indicates the sensitivity of the band i relative to the CH stretching vibration reference, which is a measure of the film amount or density. A_{CH} should remain the same, regardless of the polar group, if the films are similarly or randomly oriented.

The orientation was probed by measuring the dichroic ratio using polarized FTIR spectroscopy, as detailed before (Ahn and Franses, 1992a). As shown in Table 2, cast films (deposited directly from a solvent on the ATR plate surface) and collapsed films of different ionic compositions have ATR dichroic ratios around 0.88. For these systems, this value corresponds to random or isotropic orientation. Hence, the ionic composition is not affected by the molecular orientation of the collapsed films. With this method (Eq. 1) and Figures 1–3, one obtains: α_H^{-1} = 2.12, α_{Ca}^{-1} = 1.43, and α_{Cd}^{-1} = 1.24. The value of α_H^{-1} is comparable to 2.0 reported by Bagg et al. (1964), who used peak heights. The value of α_{Ca}^{-1} is consistent with the value of 1.5 reported by Deamer et al. (1967) for partially hydrated calcium stearate.

The deposition method does affect the molecular orientation, as expected (Table 2). To test whether the deposition method affects the ionic composition in the deposited film, we examined oriented nine-layer LB films transferred at surface pressures of 10 and 25 mN/m. The deposition method and the surface pressure made no difference in the observed composition, but did affect slightly the dichroic ratio and, thus, the orientation of the chain axis. The average chain axis tilt angle was somewhat higher than previously reported for monolayers and multilayers of cadmium stearate LB films, deposited from the subsolution without calcium ions (Outka et al., 1987; Umemura et al., 1990, Ahn and Franses, 1992a).

Model for Ion Adsorption to Thin Films

In this section, we develop the model describing competitive adsorption of ternary ions to Langmuir monolayers. The model will then be modified to supply the ionic composition of the deposited films on solid surfaces. The adsorption of ions to the fatty acid Langmuir monolayer spread on the aqueous subsolution containing various chemically-different ions is depicted in Figure 5. The array of insoluble surfactant molecules in a liquid-condensed state defines a two-dimensional lattice, as observed with AFM (atomic force microscopy) by Schwartz et al. (1992). We consider the case of constant area per surfactant molecule (and possibly variable surface pressure). Binary mixtures of protons and bivalent ions (Figure 5a) have provided information on (i) the binding constant and (ii) the mixing characteristics of the bivalent ions to protons (Ahn and Franses, 1991). Also, binary mixtures of two kinds of bivalent ions (Figure 5b) can supply us with the mixing behavior among those ions, as theoretically suggested before (Ahn and Franses, 1992b). In this study, we present a more general ion adsorption model for ternary mixtures of protons and two kinds of bivalent ions (Figure 5c) to represent the H^+-Ca^{2+}-Cd^{2+} system. Since protons are always present in aqueous solutions, it is necessary to use a ternary ionic system for examining the ion exchange between the other two ions.

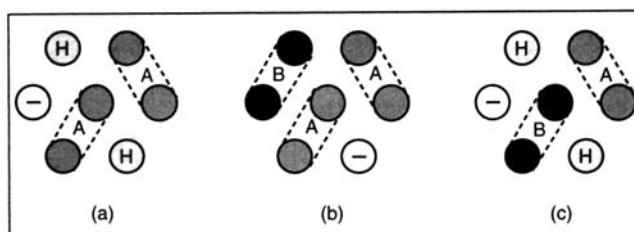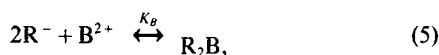The adsorption of ions (H^+, A^{2+}, and B^{2+}) to the empty
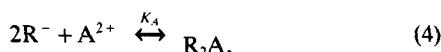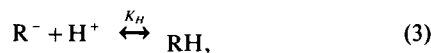

Figure 5. Ion adsorption on a lattice representing a Langmuir monolayer: (a) proton (H) and bivalent ion (A) system; (b) two kinds of bivalent ion (A, B) system; (c) proton and two kinds of bivalent ions system.

lattice sites (R^-) can be described by the following competitive "reactions":

$$R^- + H^+ \overset{K_H}{\longleftrightarrow} RH, \tag{3}$$

$$2R^- + A^{2+} \overset{K_A}{\longleftrightarrow} R_2A, \tag{4}$$

$$2R^- + B^{2+} \overset{K_B}{\longleftrightarrow} R_2B, \tag{5}$$

where K_H, K_A, and K_B are the binding constants of the ions H^+, A^{2+}, and B^{2+}, respectively. Expressing the binding constants in terms of activities, one gets:

$$a_H = K_H a_o a_H^s \tag{6}$$

$$a_A = K_A a_o^2 a_A^s \tag{7}$$

$$a_B = K_B a_o^2 a_B^s \tag{8}$$

where a_j represents the activity of the ion j adsorbed to the lattice sites; a_o represents that of the empty site R^-; a_j^s represents the solution ion activity at the subsurface adjacent to the interface or at the outer Helmholtz plane. The Flory-Huggins equation is applied to the lattice plane containing monomers (R^- and RH) and dimers (R_2A and R_2B). The Flory-

$$
\begin{bmatrix} \phi_o \\ \phi_H \\ \phi_A \\ \phi_B \end{bmatrix} = D^{-1} \begin{bmatrix} 1 \\ K_H a_H^s \exp(-\chi_{HA}\phi_A - \chi_{HB}\phi_B) \\ K_A a_A^s \phi_o \exp\{1 - 2(\chi_{HA}\phi_H + \chi_{AB}\phi_B)\} \\ K_B a_B^s \phi_o \exp\{1 - 2(\chi_{HB}\phi_H + \chi_{AB}\phi_A)\} \end{bmatrix} \tag{13}
$$

where

$$
D = 1 + K_H a_H^s \exp(-\chi_{HA}\phi_A - \chi_{HB}\phi_B)
$$
$$
+ K_A a_A^s \phi_o \exp\{1 - 2(\chi_{HA}\phi_H + \chi_{AB}\phi_B)\}
$$
$$
+ K_B a_B^s \phi_o \exp\{1 - 2(\chi_{HB}\phi_H + \chi_{AB}\phi_A)\} \tag{14}
$$

Using the ideal solution equation for solution ion activity a_j^s produces little difference from using the Debye-Hückel or other theory of nonideal solution, because of the dilute solutions involved (Ahn and Franses, 1991). Therefore, in further calculations, a_j^s has been assumed to equal the mole fraction x_j^s of the ion at the subsurface.

The lattice plane is charged due to the dissociated molecules R^-. The subsurface concentrations of the ions are thus affected by the electrostatic interactions. The Poisson-Boltzmann diffuse layer equation for the present asymmetric electrolyte solution has been solved for the electrical potential ψ in the z-direction. The result is:

$$
\frac{\psi(z)}{(k_B T/q)} = -\ln C_N + \ln \left\{ -(C_A + C_B) + I \tanh^2 \left[\frac{I^{1/2}}{2(3C_A + 3C_B)^{1/2}} \kappa z + \tanh^{-1} \left[\frac{C_A + C_B + C_N \exp\left(\frac{q\psi_o}{k_B T}\right)}{I} \right]^{1/2} \right] \right\} \tag{15}
$$

Huggins binary interaction parameters χ_{ij} describe the two-dimensional mixing behavior of the ions. As done before (Ahn and Franses, 1991), it is assumed that the interactions of adsorbed ions with empty sites are negligible compared with other interactions among ions. Thus, only χ_{HA}, χ_{HB}, and χ_{AB} are important binary interaction parameters. The activities a_j can be derived:

$$\ln a_o = \ln \phi_o + \frac{1}{2}(\phi_A + \phi_B) - \chi_{HA}\phi_H\phi_A - \chi_{HB}\phi_H\phi_B - \chi_{AB}\phi_A\phi_B \tag{9}$$

$$\ln a_H = \ln \phi_H + \frac{1}{2}(\phi_A + \phi_B) + \chi_{HA}(1 - \phi_H)\phi_A$$
$$+ \chi_{HB}(1 - \phi_H)\phi_B - \chi_{AB}\phi_A\phi_B \tag{10}$$

$$\ln a_A = \ln \phi_A - (\phi_o + \phi_H) + 2[\chi_{HA}\phi_H(1 - \phi_A)$$
$$- \chi_{HB}\phi_H\phi_B + \chi_{AB}(1 - \phi_A)\phi_B] \tag{11}$$

$$\ln a_B = \ln \phi_B - (\phi_o + \phi_H) + 2[-\chi_{HA}\phi_H\phi_A$$
$$+ \chi_{HB}\phi_H(1 - \phi_B) + \chi_{AB}\phi_A(1 - \phi_B)] \tag{12}$$

where ϕ_j is the area fraction of the component j in the Langmuir monolayer; ϕ_o is that of the vacant lattice sites. This definition is consistent with the procedure for calculating composition from IR absorbances, as given by Eq. 2. The final equations for ϕ_j are:

Here, C_j is the bulk molar concentration of the ion j; C_N is the total bulk molar concentration of anions ($C_N = C_H + 2C_A + 2C_B$); I is the ionic strength of the aqueous subsolution ($I = C_H + 3C_A + 3C_B$); k_B is the Boltzmann constant; T is the absolute temperature of the system; q is the electron charge; κ is the inverse Debye length as defined by $\kappa \equiv (2N_A q^2 I/\epsilon\epsilon_o k_B T)^{1/2}$ (in SI units), where N_A is Avogadro's number, ϵ is the dielectric constant of water, and ϵ_o is the permittivity of vacuum space. ψ_o is the surface potential at $z = 0$ and is related to ϕ_o by the following equation:

$$
q\Gamma\phi_o = - \left[1 - \exp\left(-\frac{q\psi_o}{k_B T} \right) \right]
$$
$$
\times \left[2N_A\epsilon\epsilon_o k_B T \left\{ C_A + C_B + C_N \exp\left(\frac{q\psi_o}{k_B T}\right) \right\} \right]^{1/2} \tag{16}
$$

where Γ is the surface density of the surfactant monolayer in the liquid-condensed state. The value of $\Gamma^{-1} = 0.2$ nm^2/molecule is appropriate for an oriented close-packed monolayer of a single-straight chain fatty acid. The subsurface ion concentrations C_j^s are related to C_j:

$$C_j^s = C_j \exp\left(-n_j \frac{q\psi_o}{k_B T} \right) \tag{17}$$

where n_j is the valence of the ion j. Then, the mole fraction of ions at the subsurface is:
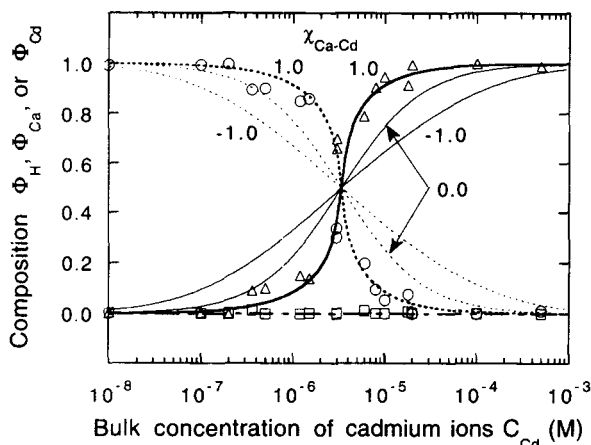
Figure 6. Dependence of ionic compositions in the films on C_{Cd}, at pH = 10 and $C_{Ca} = 10^{-4}$ M.

$\circ$ and $\cdots$, calcium salt; $\triangle$ and ——, cadmium salt; $\square$ and ----, acid. Lines: calculated results with $K_H = 3.6 \times 10^6$, $K_{Cd} = 8.6 \times 10^3$, $K_{Ca} = 2.9 \times 10^2$, $\chi_{H\text{-}Ca} = -0.76$, and $\chi_{H\text{-}Cd} = 0.13$.

$$x_j^s = \frac{C_j^s}{C_{water} + \sum_j C_j^s} \qquad (18)$$

Whereas Langmuir monolayers are partially charged, LB and collapsed films are neutralized upon deposition and subsequent evaporation of water. Moreover, unlike LB films, which are usually deposited in a fairly dry state (except water of hydration), the deposition of collapsed films may involve an appreciable amount of water entrained on the ATR plates. Evaporation of this water leads to neutral films mixed with salts crystallized from the small amount of entrained bulk solution. These salts, which are not bound to the surfactant polar groups, are not detectable by IR spectroscopy and are of little importance here, since the model concerns the ions bound to the Langmuir monolayers. Most of the spread monolayer sites are covered by ions. After drying, all the remaining sites are covered. For directly comparing composition results using the IR spectra of dried films to the model, which deals with a Langmuir monolayer, the ϕ_j values should be corrected for the additional ion binding accompanying drying. Collapsed films are expected to be further neutralized by the additional ion adsorption during drying after deposition as well as during the collapsed process. A reasonable estimate of a composition correction is based on the idea that the additional ion adsorption is determined by the relative concentrations and the binding constants of the ions in the diffuse layer ($K_j\Gamma_j$). Then, the composition Φ_j of the collapsed-and-dried films can be given:

$$\Phi_j = \phi_j + \frac{n_j K_j \Gamma_j}{\sum_j n_j K_j \Gamma_j} \phi_o \qquad (19)$$

where Γ_j is the integrated ion concentration over the length of the diffuse layer from $z = 0$ to $10 \ \kappa^{-1}$ and is obtained by:

$$\Gamma_j = \int_0^{10\kappa^{-1}} C_j \exp\left[-n_j \frac{q\psi(z)}{k_B T} \right] dz \qquad (20)$$

Calculated values of Φ_j were not sensitive to the value of the upper limit in Eq. 20. Most of the corrections amounted to less than 10%. The model-predicted compositions Φ_j (Eq. 19) will be compared to the spectroscopic compositions Φ_i (Eq. 2) for the H^+-Ca^{2+}-Cd^{2+} system in the subsequent section.

Ion Exchange in Thin Films

Parameter determination from binary ionic systems

To calculate the ionic compositions from the model for the system containing H^+, Ca^{2+}, and Cd^{2+} ions, we need to know the parameter values of K_H, K_{Ca}, K_{Cd}, $\chi_{H\text{-}Ca}$, $\chi_{H\text{-}Cd}$, and $\chi_{Ca\text{-}Cd}$. Ahn and Franses (1991) obtained the following values for the first five parameters by fitting the binary ion model to experimental data: $K_H = 3.63 \times 10^6$, $K_{Ca} = 2.9 \times 10^2$, $K_{Cd} = 8.6 \times 10^3$, $\chi_{H\text{-}Ca} = -0.76$, and $\chi_{H\text{-}Cd} = 0.13$. The value for $\chi_{Ca\text{-}Cd}$ can be obtained, in principle, for the system consisting of calcium and cadmium ions. Even though aqueous solutions always involve protons, at a high pH a pseudobinary calcium-cadmium system may be achieved. Then $\chi_{Ca\text{-}Cd}$ can be calculated. Compositions were obtained for different bulk concentrations of cadmium ions (10^{-8} to 5×10^{-4} M), at $C_{Ca} = 10^{-4}$ M and pH = 10 (Figure 6). At pH = 10, the acid area fraction was found to be close to zero, which indicated that the system was effectively binary. Binary model calculations fit the data well with one adjustable parameter, $\chi_{Ca\text{-}Cd} = 1.0 \pm 0.2$, and with two fixed parameters K_{Ca} and K_{Cd}, which were previously determined. This positive χ value indicates that calcium and cadmium ions do not mix well with each other ($\chi_{Ca\text{-}Cd} > 0$). The consequence is that the breakthrough curve is steep, as found. Had $\chi_{Ca\text{-}Cd}$ been lower, ions would mix better and the ion exchange would occur in the wider range of C_{Cd}, as shown in Figure 6.

Model calculations show another interesting engineering point. At the middle point of the breakthrough curves, where $\Phi_{Ca} = \Phi_{Cd}$, one finds that $K_{Ca}C_{Ca} \simeq K_{Cd}C_{Cd}$, regardless of the value of $\chi_{Ca\text{-}Cd}$. The quantity $K_j C_j$, rather than K_j, represents the apparent binding capacity of the ion j and has a simple interpretation. The major component of the films can be determined simply by comparing these apparent binding capacities of the ions with the *same* valence. This simple measure of the ion binding capacity provides one with insight on the ion exchange among several bivalent metal ions. This rule is not valid for mixtures of ions of *different* valence, as one can attest from many examples and confirm by inspecting Eqs. 13 and 19. In such cases, one should additionally consider the effects of electrical double layer and χ parameters.

Ion exchange in ternary ionic system of H^+-Ca^2-Cd^{2+}

A large number of IR spectra have been taken at increasing bulk cadmium concentration and at $C_{Ca} = 5 \times 10^{-4}$ M and pH = 5.5. Representative spectra and spectral analysis results are given in Figure 7. When $C_{Cd} = 0$, one obtains from the top spectrum $\Phi_H = 0.79$ and $\Phi_{Ca} = 0.21$ (Eq. 2). The composition remains unchanged for C_{Cd} up to about 10^{-6} M. In the range from $C_{Cd} = 2 \times 10^{-6}$ to 10^{-5} M, Φ_H increases to about 0.85 and accompanies a corresponding decrease in Φ_{Ca} but no change in Φ_{Cd}, as shown in Figure 8. This change, although small in magnitude, is reproducible and, we believe, significant compared to experimental error. Thus, the addition of cadmium ions makes some exchange of the adsorbed calcium ions by
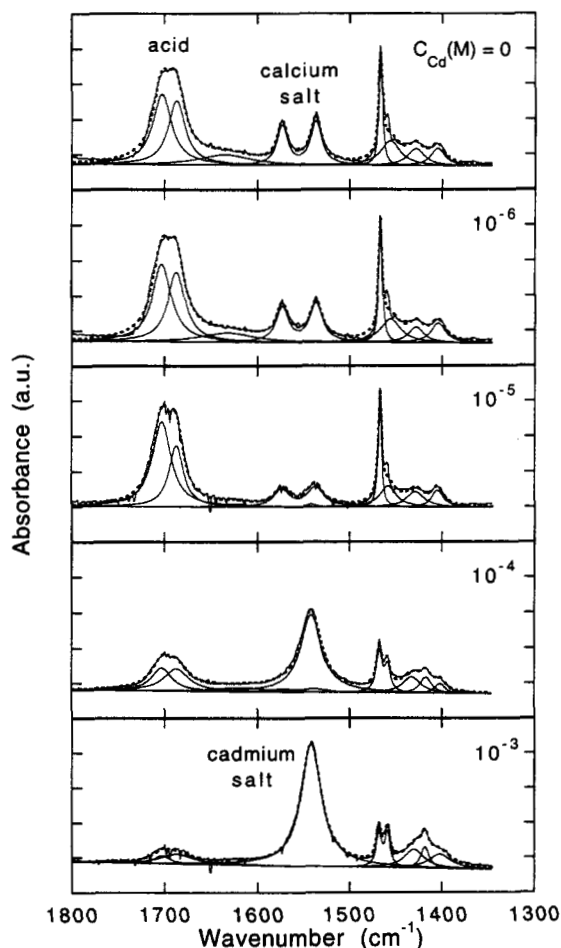
Figure 7. FTIR spectra of mixed-ion films at pH = 5.5 and $C_{Ca} = 5 \times 10^{-4}$ M and increasing C_{Cd}.

Spectral fits were used to calculate compositions; cadmium salt is evident for $C_{Cd} > 10^{-5}$ M.
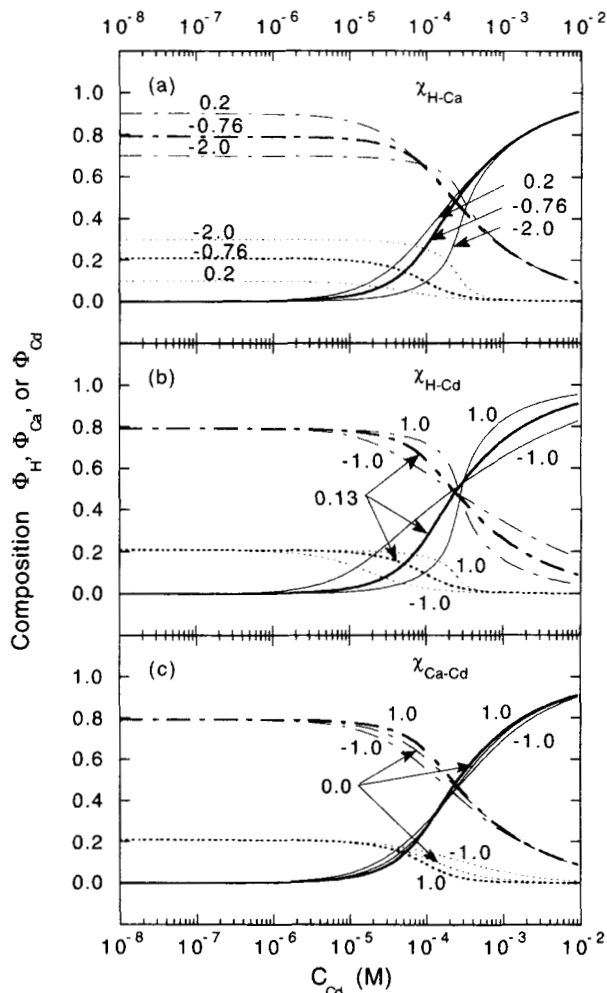

Figure 9. Effects of binary interaction parameters (a) χ_{H-Ca}, (b) χ_{H-Cd}, and (c) χ_{Ca-Cd} on ion exchange.

Parameter values were chosen to be the same as in Figure 8, unless indicated otherwise.
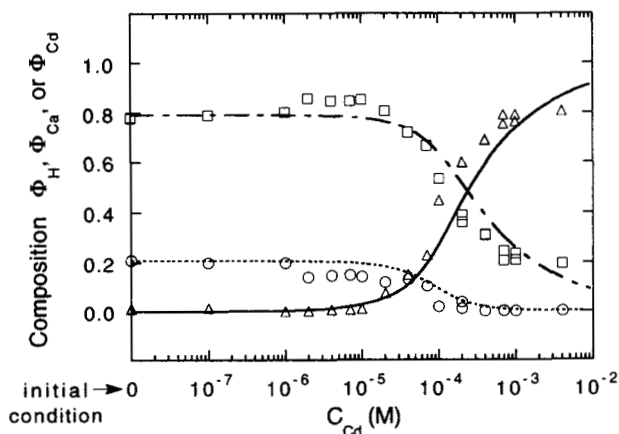

Figure 8. Comparison of model predictions and data on ternary ionic compositions of the films, at the same conditions as in Figure 7.

o and ····, calcium salt; △ and ——, cadmium salt; □ and ---, acid. Model predictions were made with $\chi_{Ca-Cd} = 1.0$ determined in Figure 7 and other parameters values, as used in Figure 6. The uncertainty of the data points is about the size of the symbols.

protons. For $C_{Cd} > 2 \times 10^{-5}$ M, both protons and calcium ions are gradually exchanged by cadmium ions. At $C_{Cd} > 10^{-4}$ M no calcium salt is detected, and for $C_{Cd} \geq 10^{-3}$ M the acid component is minor. Predicted compositions based on a ternary model using parameters determined from binary ionic systems (see previous subsection) compare well with the data, except for the slight rise in Φ_H at $C_{Cd} = 2 \times 10^{-6}$ to 10^{-5} M. This rise may be due to ternary ionic interactions, which are not accounted in the model.

To obtain some further insight into the effect of the χ parameters on the ionic compositions, we have done sample calculations for hypothetical values of χ. Figure 9 shows that as the parameter χ_{H-Ca} decreases, Φ_{Ca} would normally increase, because apparently calcium ions would be better mixed with protons. This would result in suppression of the ion exchange by cadmium ions (Figure 9a). By contrast, had the parameter χ_{H-Cd} been smaller, calcium ions would be more easily replaced by cadmium ions: Φ_{Ca} would decrease to one-half of its initial value of 0.21 at $C_{Cd} \approx 10^{-5}$ M when χ_{H-Cd} is -1.0, and at $C_{Cd} \approx 2 \times 10^{-4}$ M when χ_{H-Cd} is $+1.0$ (Figure 9b). With a smaller χ_{H-Cd}, the complete ion exchange process would occur over a

Table 3. Effect of Interaction Parameter on Predicted Compositions at Various pH Values for Binary Proton-Bivalent Ion Systems

C_{Ca} (M)	χ_{H-Ca}	pH = 5.5		pH = 6.0		pH = 7.0	
		Φ_H	Φ_{Ca}	Φ_H	Φ_{Ca}	Φ_H	Φ_{Ca}
10^{-4}	0.2	0.90	0.10	0.83	0.17	0.16	0.84
10^{-4}	-0.76	0.79	0.21	0.72	0.28	0.23	0.77
10^{-4}	-2.0	0.70	0.30	0.65	0.35	0.31	0.69
C_{Cd} (M)	χ_{H-Cd}	Φ_H	Φ_{Cd}	Φ_H	Φ_{Cd}	Φ_H	Φ_{Cd}
10^{-4}	1.0	0.79	0.21	0.16	0.84	0.01	0.99
10^{-4}	0.13	0.63	0.37	0.26	0.74	0.03	0.97
10^{-4}	-1.0	0.57	0.43	0.34	0.66	0.07	0.93

wider range of bulk cadmium ion concentration. Finally, had χ_{Ca-Cd} been smaller, protons would be replaced slightly more easily by cadmium ions (Figure 9c). In this case, calcium ions are exchanged over a wider range of cadmium ion concentration.

Table 3 shows the dependence on pH of the effects of mixing parameters on the ionic compositions of binary systems. At pH = 5.5, Φ_{Ca} (or Φ_{Cd}) would increase as χ_{H-Ca} (or χ_{H-Cd}) decreases (negative effect). By contrast, at pH = 7.0, Φ_{Ca} (or Φ_{Cd}) would decrease as the mixing parameter decreases (positive effect). In the intermediate pH region (pH = 6.0), however, the mixing parameter has different effects on Φ_{Ca} and Φ_{Cd}: as χ decreases, Φ_{Ca} increases (negative effect) but Φ_{Cd} decreases (positive effect). Therefore, the values of χ_{H-Ca} and χ_{H-Cd} have different implications on mixing and exchange, depending on the pH and ion concentrations.

Discussion

The results presented here are useful for accurately describing and controlling the ionic composition of monolayers, and the deposition quality of resulting LB films. Potential uses of thin films as ion exchange materials are also suggested. Heavy toxic ions, such as cadmium or lead, can be removed from dilute aqueous solutions by using fatty acid films. The approach used here may be useful for understanding ion exchange with resins containing surface carboxylic groups in packed-bed ion exchangers. Moreover, if the ion exchange effect can be detected *in situ*, then LB film configurations could also lead to ion-sensing applications.

Conclusions

• The compositions of fatty acid collapsed and ordered LB films, deposited at different surface pressures of 10 and 25 mN/m, are independent of orientation and surface pressure, and depend on the bulk concentrations of ions (H^+, Ca^{2+}, and Cd^{2+}).

• FTIR ATR spectroscopy can be used to independently examine the acid, calcium salt, and cadmium salt fractions in the films deposited on ATR plates. The ionic compositions in the films can be obtained by analyzing IR absorbance spectra.

• A ternary ion equilibrium adsorption model has been developed and includes the effects of the ion binding constants at the interface and binary interaction parameters describing ions mixing in the two-dimensional lattice space. The model predicts the ternary ionic composition data very well, with parameters determined from binary ionic systems.

Acknowledgment

Notation

a_o = activity of vacant lattice site
a_j = activity of adsorbed j-ion (j = H, Ca, or Cd)
a_j^s = solution ion activity at subsurface (outer Helmholtz plane)
A_i = integrated absorbance of IR band i (i = CH for CH stretching band, H for C = O stretching band, Ca for asymmetric COO-Ca stretching band, or Cd for asymmetric COO-Cd stretching band)
C_j = bulk ion concentration, M (mol·L^{-1})
C_j^s = subsurface ion concentration, M
C_N = total bulk concentration of anions, M
D = denominator as defined by Eqs. 13 and 14
I = ionic strength of aqueous subsolution, M
k_B = Boltzmann constant = 1.381×10^{-23} J·K^{-1}
K_j = ion binding constant, dimensionless
n_j = ion valence
N_A = Avogadro's number = 6.022×10^{23} mol^{-1}
q = electron charge = 1.602×10^{-19} C
T = absolute temperature, K
x_j^s = mole fraction of ion at subsurface
z = distance from subsurface through subsolution, m

Greek letters

α_i = sensitivity factor of IR band i relative to CH stretching band
Γ = surface density of liquid-condensed monolayer
Γ_j = integrated ion concentration in electrical diffuse layer
ϵ = dielectric constant of water
ϵ_o = permittivity of vacuum = 8.854×10^{-12} kg^{-1}·m^{-3}·s^4·A^2
κ = inverse Debye length, m^{-1}
ϕ_j = area fraction of ion j with Langmuir monolayers
ϕ_o = area fraction of vacant lattice site
Φ_i = ionic composition as measured by IR spectroscopy
Φ_j = ionic composition, as calculated by model (Eq. 19)
χ_{ij} = Flory-Huggins binary interaction (or mixing) parameter
$\psi(z)$ = electrical potential, V

Subscripts

i, j = ion or IR band corresponding to ion
o = vacant lattice site

Superscripts

s = subsurface

Literature Cited

Ahn, D. J., and E. I. Franses, "Interactions of Charged Langmuir Monolayers with Dissolved Ions," *J. Chem. Phys.*, 95, 8486 (1991).

Ahn, D. J., and E. I. Franses, "Orientations of Chain Axes and Transition Moments in Langmuir-Blodgett Monolayers Determined by Polarized FTIR-ATR Spectroscopy," *J. Phys. Chem.*, 96, 9952 (1992a).

Ahn, D. J., and E. I. Franses, "Compositions of Langmuir Monolayers and Langmuir-Blodgett Films with Mixed Counterions," *ACS Symp. Ser.*, 501, 342 (1992b).

Bagg, J., M. B. Abramson, M. Fichman, M. D. Haber, and H. P. Gregor, "Composition of Stearic Acid Monolayers from Calcium-Containing Substrates," *J. Am. Chem. Soc.*, 86, 2759 (1964).

Bloch, J. M., and W. Yun, "Condensation of Monovalent and Divalent Metal Ions on a Langmuir Monolayer," *Phys. Rev. A*, 41, 844 (1990).

Bruinsma, P. J., G. J. R. Spooner, L. B. Coleman, R. Koren, C. Sturesson, and P. Stroeve, "Selectivity of Toxic and Acid Gases over Methane and Nitrogen in LB Films," *Thin Solid Films*, 210/211, 440 (1992).

Chapman, D., "Biomembranes and New Hemocompatible Materials," *Langmuir*, 9, 39 (1993).

Deamer, D. W., D. W. Meek, and D. G. Cornwell, "Properties, Composition, and Structure of Stearic Acid-Stearate Monolayers on Alkaline Earth Solutions," *J. Lipid Res.*, 8, 255 (1967).

Dluhy, R. A., and D. G. Cornell, "*In Situ* Measurement of the Infrared Spectra of Insoluble Monolayers at the Air-Water Interface," *J. Phys. Chem.*, 89, 3195 (1985).

Fox, M. A., W. E. Jones, Jr., and D. M. Watkins, "Light-Harvesting Polymer Systems," *C&EN*, 71(11), 38 (1993).

Hua, Y. L., D. P. Jiang, Z. Y. Shu, M. C. Petty, G. G. Roberts, and M. M. Ahmad, "Substituted Silicon Phthalocyanine Langmuir-Blodgett Film and Its Possible Use in Electronic Devices," *Thin Solid Films*, 192, 383 (1990).

Jain, T. K., M. Varshey, and M. Maitra, "Structural Studies of Aerosol OT Reverse Micellar Aggregates by FTIR Spectroscopy," *J. Phys. Chem.*, 93, 7409 (1989).

Kimura, F., J. Umemura, and T. Takenaka, "FTIR-ATR Studies on Langmuir-Blodgett Films of Stearic Acid with 1-9 Monolayers," *Langmuir*, 2, 96 (1986).

Kobayashi, K., K. Takaoka, and S. Ochiai, "Application of X-Ray Photoelectron Spectroscopy and Fourier Transform IR-Reflection Absorption Spectroscopy to Studies of the Composition of Langmuir-Blodgett Films," *Thin Solid Films*, 159, 267 (1988).

Kuan, S. W. J., C. W. Frank, C. C. Fu, D. R. Allee, P. Maccagno, and R. F. W. Pease, "Ultrathin Polymer Films for Microlithography," *J. Vac. Sci. Technol. B*, 6, 2274 (1988).

Lösche, M., C. Helm, H. D. Mattes, and H. Möhwald, "Formation of Langmuir-Blodgett Films via Electrostatic Control of the Lipid/Water Interface," *Thin Solid Films*, 133, 51 (1985).

Marshbanks, T. L., H. K. Jugduth, W. N. Delgass, and E. I. Franses, "Structure and Composition of LB Films of Cadmium Stearate by FTIR Spectroscopy and XPS," *Thin Solid Films*, 232, 126 (1993).

McLaughlin, S., N. Mulrine, T. Gresalfi, G. Vaio, and A. McLaughlin, "Adsorption of Divalent Cations to Bilayer Membranes Containing Phosphatidylserine," *J. Gen. Physiol.*, 77, 445 (1981).

Moriizumi, T., "Langmuir-Blodgett Films as Chemical Sensors," *Thin Solid Films*, 160, 413 (1988).

Outka, D. A., J. Stöhr, J. P. Rabe, J. D. Swalen, and H. H. Rotermund, "Orientation of Arachidate Chains in Langmuir-Blodgett Monolayers on Si(111)," *Phys. Rev. Lett.*, 59, 1321 (1987).

Petrov, J. G., I. Kuleff, and D. Platikanov, "Neutron Activation Analysis of Metal Ions in Langmuir-Blodgett Multilayers of Arachidic Acid," *J. Colloid Interface Sci.*, 88, 29 (1982).

Pezron, E., P. M. Claesson, J. M. Berg, and D. Vollhardt, "Stability of Archidic Acid Monolayers on Aqueous Salt Solutions," *J. Colloid Interface Sci.*, 138, 245 (1990).

Rabolt, J. F., F. C. Burns, N. E. Schlotter, and J. D. Swalen, "Anisotropic Orientation in Molecular Monolayers by Infrared Spectroscopy," *J. Chem. Phys.*, 78, 946 (1983).

Roberts, G., ed., *Langmuir-Blodgett Films*, Plenum Press, New York (1990).

Schwartz, D. K., J. Garnaes, R. Viswanathan, and J. A. N. Zasadzinski, "Surface Order and Stability of Langmuir-Blodgett Films," *Sci.*, 257, 508 (1992).

Stroeve, P., and E. Franses, eds., *Molecular Engineering of Ultrathin Polymeric Films*, Elsevier Press, London (1987).

Swalen, J. D., "Optical Properties of Langmuir-Blodgett Films," *J. Molec. Electronics*, 2, 155 (1986).

Swalen, J. D., D. L. Allara, J. D. Andrade, E. A. Chandross, S. Garoff, J. Israelachvili, T. J. McCarthy, R. Murray, R. F. Pease, J. F. Rabolt, K. J. Wynne, and H. Yu, "Molecular Monolayers and Films," *Langmuir*, 3, 932 (1987).

Ulman, A., *An Introduction to Ultrathin Organic Films: From Langmuir-Blodgett to Self-Assembly*, Academic Press, New York (1991).

Umemura, J., T. Kamata, T. Kawai, and T. Takenaka, "Quantitative Evaluation of Molecular Orientation in Thin Langmuir-Blodgett Films by FT-IR Transmission and Reflection-Absorption Spectroscopy," *J. Phys. Chem.*, 94, 62 (1990).

Vogel, C., J. Corset, and M. Dupeyrat, "Etude par Spectroscopie Infrarouge de la Structure de Couches de Langmuir-Blodgett: I. Couches d'Acide Stearique et de Stearate de Plomb," *J. Chim. Phys.*, 76, 903 (1979).

Whitesides, G. M., and P. E. Laibinis, "Wet Chemical Approaches to the Characterization of Organic Surfaces: Self-Assembled Monolayers, Wetting, and the Physical-Organic Chemistry of the Solid-Liquid Interface," *Langmuir*, 6, 87 (1990).

Williams, D., "Polymers in Nonlinear Optics," *Adv. Chem. Ser.*, 218, 297 (1988).

Wohltjen, H., W. R. Barger, A. W. Snow, and N. L. Jarvis, "A Vapor-Sensitive Chemiresistor Fabricated with Planar Microelectrodes and a Langmuir-Blodgett Organic Semiconductor Film," *IEEE Trans. on Electron Devices*, ED-32, 1170 (1985).

Yamauchi, A., A. Matsubara, H. Kimizuka, and L. G. Abood, "Differential Effect of Sodium and Potassium on Calcium Adsorption to Stearic Acid Monolayers," *Biochim. Biophys. Acta*, 150, 181 (1968).